

INTERNATIONAL SOCIETY FOR SOIL MECHANICS AND GEOTECHNICAL ENGINEERING



This paper was downloaded from the Online Library of the International Society for Soil Mechanics and Geotechnical Engineering (ISSMGE). The library is available here:

<https://www.issmge.org/publications/online-library>

This is an open-access database that archives thousands of papers published under the Auspices of the ISSMGE and maintained by the Innovation and Development Committee of ISSMGE.

The paper was published in the proceedings of the 11th Australia New Zealand Conference on Geomechanics and was edited by Prof. Guillermo Narsilio, Prof. Arul Arulrajah and Prof. Jayantha Kodikara. The conference was held in Melbourne, Australia, 15-18 July 2012.

Study on Variations of Stiffness during Multiple-step Loading Test on a Cement-mixed Gravel

A. Taheri¹, F. Tatsuoka²

¹ School of Civil, Environmental and Mining Engineering, The University of Adelaide, Adelaide, South Australia 5005; PH (+61) 8- 8313-0906; FAX (+61) 8-8303-4359; email: abbas.taheri@adelaide.edu.au

² Department of Civil Engineering, Tokyo University of Science, Japan, PH (81) 4-7124-1501; FAX (81) 4-7123-9766; email: tatsuoka@rs.noda.tus.ac.jp

ABSTRACT

Effects of intermediate loading histories, with large stress-amplitude unload/reload cycles, on the stiffness of compacted cement-mixed well-graded gravelly soil in a multiple-step loading (ML) drained TC test using a single specimen were evaluated. ML tests were conducted following both increasing and decreasing confining pressures (σ_h s). A set of single-step loading (SL) tests at different σ_h s were also performed. Large-strain stiffness variations in terms of Tangent Young's modulus, E_{tan} , were investigated. E_{tan} was affected by three factors: a) E_{tan} value increased at the same stress state by cyclic loading due to the elasto-viscoplastic properties (CL effect); b) E_{tan} value altered with confining pressure level (P effect): b-1) A decrease in the E_{tan} value at the same shear stress ratio, q/q_{max} , value, as well as an increase in the strain at the peak stress state and an increase in the post-peak ductility, with an increase in σ_h s. This effect is relevant only for the stress-strain behaviour during primary loading. b-2) An increase (a decrease) in the E_{tan} value at the same q/q_{max} value with an increase (a decrease) in σ_h s. This effect is relevant only for the stress-strain behaviour during reloading; c) E_{tan} value decreased due to damage to the structure by irreversible shearing at previous loading and negative irreversible shearing during unloading (D effect). In increasing σ_h test, CL effect was masked by P effect and D effect was negligible. However, in decreasing σ_h test, D effect was more significant. Large damage effect in decreasing σ_h test was also observed in small-strain stiffness values.

Keywords: Multiple-step loading, triaxial compression test, Cement-mixed gravel, Stiffness,

1 INTRODUCTION

Use of backfill of highly-compacted cement-mixed gravel (CMG) as a bridge abutment started in 2003, at Takada for a Shinkansen train line in Kyushu, Japan (Aoki et al. 2003, Watanabe et al. 2003, Tatsuoka et al. 2004). Until today, more than fifty similar bridge abutments were constructed or decided to be constructed in Japan. This experience showed high performance of CMG in such permanent civil engineering structures.

CMG may be subjected to a wide variety of loading histories, including cyclic loading and changes in the confining pressure, prior to a given concerned final loading history. For example, cyclic loading in the vertical direction takes place by traffic loads in the CMG backfill of retaining wall structures or bridge abutments and randomly during seismic events. More specifically, the CMG backfill of an integrated bridge (Tatsuoka et al. 2009) is subjected to horizontal cyclic loading due to seasonal thermal expansion and construction of the girder. A number of experimental works were performed to study a wide variety of pre-loading history on the stress-strain properties of unbound geomaterials (i.e., clays, sands and gravels: e.g., Jovicic & Coop, 1997; Wang & Ng, 2005; Fortuna et al., 2006). On the other hand, such studies as above are very limited with rocks because of relatively small effects of pre-shearing on rather reversible pre-peak stress-strain behaviour. Tatsuoka et al. (2003) studied the effects of small number of loading cycles on a sedimentary soft rock. They found that the loading history changes the stress-strain relations due to development of residual strain caused by viscous properties.

In this paper, the effect of loading history on stiffness of CMG is studied during a series of multiple-step loading tests. Multiple-step loading (ML) triaxial compression (TC) test permits determination of a failure envelope by testing a single rock/soil specimen in a series of consolidation and shearing stages. This technique allows determination of strength parameters from fewer specimens than does conventional triaxial testing, which requires three or more specimens to determine a failure envelope

(Anderson 1974, Kovari and Tisa 1975). In ML test, it is assumed that the deformation characteristics should only be measured in the first loading step (JGS 2001). However, the variations of stiffness in the following loading steps have not been discussed in the literatures. Moreover, the effect of confining pressure on stiffness is found to be difference in different kind of material (Tatsuoka et al, 1993). Specially, the effect of stepwise increase or decrease of confining pressure in ML test is not known yet.

This paper reports results from a series of SL and ML drained TC tests. ML TC tests, were performed, following an increase or decrease in the confining pressure to proceed to the next shear loading step. The effects of different loading histories on the large-strain stiffness and small-strain stiffness at respective steps in the ML tests were studied.

2 MATERIAL AND TEST METHOD

A well-graded quarry gravel of sandstone was sieved to remove particles larger than 10 mm. Each specimen was prepared by mixing cement-to-gravel ratio by weight ($c/g = 2.5\%$) and then with a relevant amount of water. The mixture was compacted manually to produce rectangular prismatic specimens (72 mm x 72 mm in cross-section and 150 mm high). Each specimen was cured totally for 9 days under the atmospheric pressure.

A fully automated triaxial testing system was used. Displacement-controlled axial loading was applied by using a precision gear system. The confining pressure was applied by using a pneumatic loading system. Prescribed loading histories were applied in an automated way. A high pressure triaxial cell with a cell pressure capacity of 3 MPa was used. Axial strains were sensitively and accurately measured by using a pair of 160 mm-long LDTs (Goto et al., 1991). Lateral strains were measured locally by lateral LDTs. The axial strain rate, which was obtained from the displacement rates of the loading piston, was kept constant equal to 0.03%/min.

The following series of CD TC tests were performed: 1) Single-step loading (SL) TC tests at different constant confining pressure (σ_h) were performed. The specimen was isotropically consolidated at σ_h equal to 0.02, 0.50, 1.00 or 1.50 MPa before the start of continuous drained TC toward ultimate failure to determine the original stress-strain properties at constant σ_h that are free from any effects of previous loading history at the same or other confining pressures. Ten cycles of minute unload/reload were applied at many intermediate stages during otherwise continuous TC loading to evaluate quasi-elastic properties during TC loading; 2) Multiple-step loading (ML) tests were performed in a step-wise manner at $\sigma_h = 0.02, 0.25, 0.50, 0.75$ and 1.0 MPa following increasing and decreasing σ_h s with full unloading. In these ML tests, TC loading was stopped and the loading was reversed based on such a criterion that full shearing of the specimen at five loading steps under five different confining pressures within the measurement range of axial LDTs (about 2.5%) becomes feasible. In each loading step, TC loading was stopped after some large irreversible deformation has taken place either when the peak strength state was being approached during strain-hardening or after the peak strength state has been passed during strain-softening.

3 TEST RESULTS

Figure 1 shows the relationships between the deviator stress q and the axial strain ε_a from four SL drained TC tests at different σ_h s. At the lowest σ_h ($= 0.02$ MPa), significant strain-softening takes place after the peak stress state is reached at a relatively small axial strain. With an increase in σ_h , the axial strain at the peak stress state increases. These stress-strain properties are used as the reference for the stress-strain relations in the ML tests.

Figures 2a and b show the results from a pair of ML test increasing and decreasing σ_h with full unloading of q . After having passed a large-scale yield point at the second and subsequent steps, the stress-strain relation tends to rejoin the original relation at respective σ_h s as obtained from the SL tests. In Figure 2a, the stress-strain behavior during the primary loading at $\sigma_h = 0.02$ MPa, as well as those after the start of large scale yielding at the later steps at higher σ_h s, all exhibit strain-hardening until the end of TC loading. That is, at all the steps, TC loading was terminated before reaching respective peak stress states. Correspondingly, the maximum deviator stress q_{max} at each step

increases with an increase in σ_h . In Figure 2b, on the other hand, despite a decrease in σ_h , the maximum deviator stress (q_{max}) at the second step ($\sigma_h = 0.75$ MPa) is larger than that at the first step ($\sigma_h = 1.0$ MPa). This is due to that, at the first step, loading was terminated far before the peak stress state was reached during strain-hardening and, at the second step, the strain-hardening regime continues for some large axial strain increment after the start of large-scale yielding. Moreover, at the third and subsequent steps, the stress-strain behavior exhibits noticeable trends of strain-softening after the start of large-scale yielding.

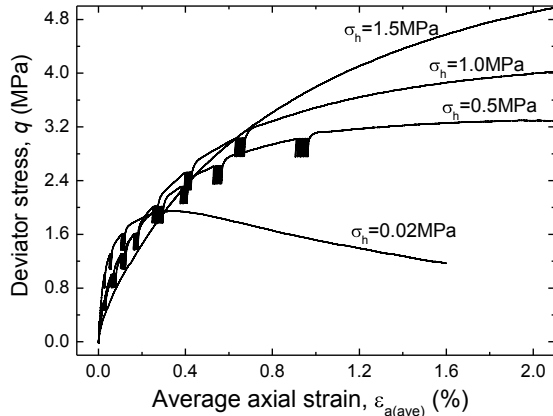


Figure 1. Summary of deviator stress - axial strains relations from SL TCs

4 EFFECT OF LOADING HISTORY ON LARGE-STRAIN STIFFNESS

The effects of loading history with changes in the confining pressure on the stress-strain properties in ML tests were studied. The tangent Young's modulus, E_{tan} , during shearing was evaluated from stress-strain relations in the single-step loading (SL) tests and the ML tests. The relationships between E_{tan} and the shear stress ratio, q/q_{max} , in the SL tests

at $\sigma_h = 0.02, 0.50, 1.00, 1.50$ MPa are plotted in Figure 3a. The similar relationships from ML tests increasing and decreasing σ_h are shown in Figures 3b and c, respectively.

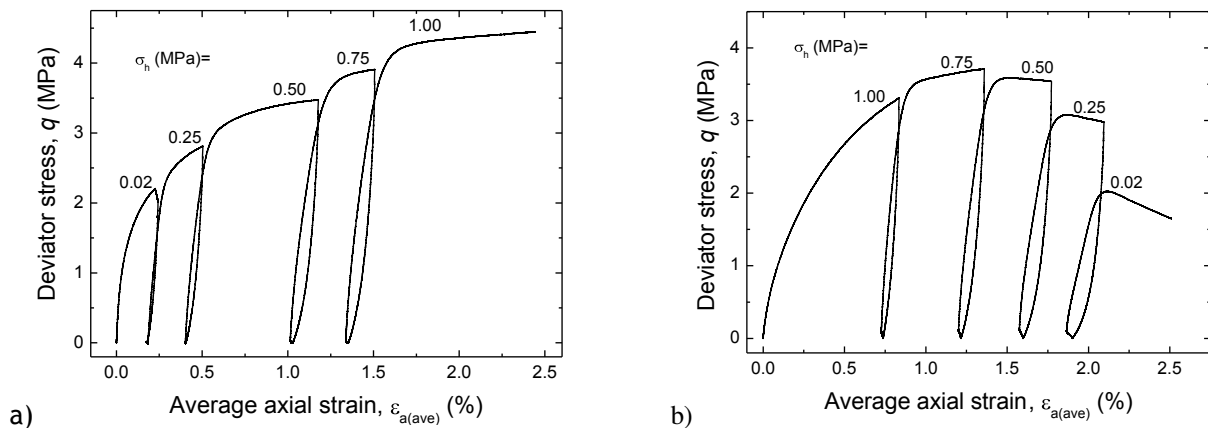


Figure 2. Deviator stress-axial relation: a) ML test increasing σ_h ; b) ML test decreasing σ_h

The continuous degradation of E_{tan} with shear deformations can be clearly seen in both SL and ML tests. In Figure 3a, (for the SL tests) the E_{tan} value at the same q/q_{max} decreases with an increase in the confining pressure. On the other hand, In Figures 3b and c (for the ML tests), the manner of the changes in the the E_{tan} value at the same q/q_{max} value with an increase in the confining pressure is much more complicated. This trend is due to combined effects on the E_{tan} value of the following three factors:

a) An increase in the E_{tan} value at the same stress state by cyclic loading due to the elasto-viscoplastic properties (CL effect). That is, the tangent stiffness during a reloading becomes larger than during the primary loading, which is relevant not only when the yield locus expands in the strain-hardening regime but also when the yield locus shrinks in the strain-softening regime.

b) Effect of pressure level:

b-1) A decrease in the E_{tan} value at the same q/q_{max} value, as well as an increase in the strain at the peak stress state and a increase in the post-peak ductility, with an increase in the confining pressures (pressure level effects; P-1 effect). This P-1 effect is relevant only for the stress-strain behaviour during a primary loading.

b-2) An increase (a decrease) in the E_{tan} value at the same q/q_{max} value with an increase (a decrease) in the confining pressures (pressure level effects; P-2 effect). This P-2 effect is relevant only for the stress-strain behaviour during a reloading, which is much more reversible than the one during a primary loading.

c) A decreases in the E_{tan} value due to damage to the structure (in particular bonding at inter-particle contact points) by irreversible shearing at previous loading (in particular those that have entered into the strain-softening regime) and negative irreversible shearing during unloading (damage effect; D effect).

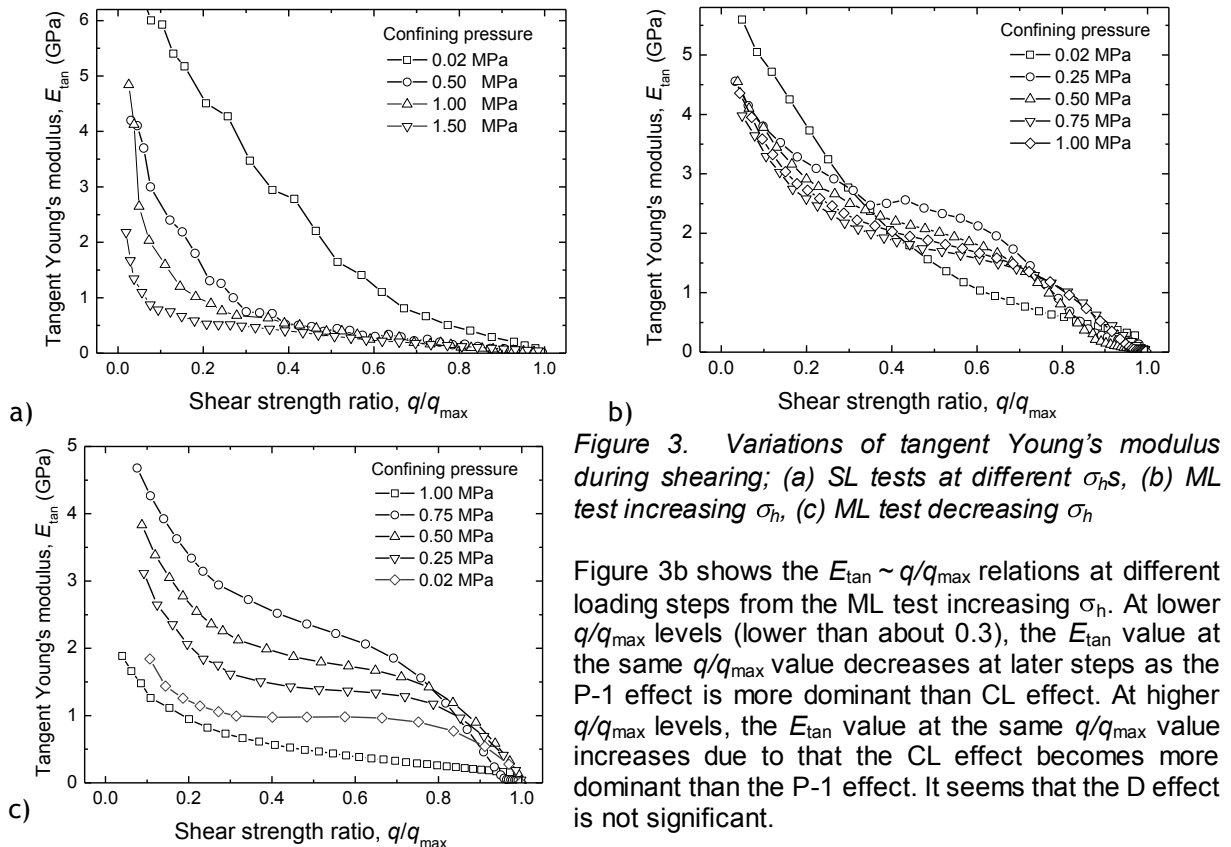


Figure 3. Variations of tangent Young's modulus during shearing; (a) SL tests at different σ_h,s , (b) ML test increasing σ_h , (c) ML test decreasing σ_h

Figure 3b shows the $E_{tan} \sim q/q_{max}$ relations at different loading steps from the ML test increasing σ_h . At lower q/q_{max} levels (lower than about 0.3), the E_{tan} value at the same q/q_{max} value decreases at later steps as the P-1 effect is more dominant than CL effect. At higher q/q_{max} levels, the E_{tan} value at the same q/q_{max} value increases due to that the CL effect becomes more dominant than the P-1 effect. It seems that the D effect is not significant.

Figure 3c shows the $E_{tan} \sim q/q_{max}$ relations at different loading steps from the ML test decreasing σ_h . At all q/q_{max} levels, the E_{tan} value at the same q/q_{max} at the second step at $\sigma_h = 0.75$ MPa is higher than the one at the first step at $\sigma_h = 1.00$ MPa. This trend is due to CL effect that is much more dominant than D effect. In this case, P-1 and P-2 effects are masked. At later steps, the E_{tan} value at the same q/q_{max} value becomes smaller. This is due to that D effect and P-2 effect become more dominant than an increase in the CL effect with an increase in the number of loading cycles.

In Figures 4a-e, the variations of the tangent Young's modulus, E_{tan} of ML tests with full unloading in increasing and decreasing σ_h , at each loading steps, are compared along together. It may be seen from Figure 4a, which demonstrates the results for $\sigma_h = 0.02$ MPa, that if any D effect were not included, E_{tan} values in the ML test decreasing σ_h should become higher than those by the first-hand loading in the ML increasing σ_h due to CL effect. At the initial stage, the actual trend is opposite, which is due likely to dominant D effect in the ML test decreasing σ_h . It seems that, as mentioned earlier for Figure 3c, during TC loading in the ML test decreasing σ_h , CL effect becomes less important but D effect becomes noticeable. In Figure 4b, a similar trend as those in the tests at $\sigma_h = 0.02$ MPa may be seen, but the trend is less obvious due likely to that the D effect in the ML test decreasing σ_h at $\sigma_h = 0.25$ MPa is smaller than the ML test decreasing σ_h at $\sigma_h = 0.02$ MPa. As shown in Figure 3c, at $\sigma_h = 0.50$ MPa, (3rd loading step in both tests), similar CL effect and D effect are exhibited in two tests. In may be seen from Figure 4d that, in the ML test increasing σ_h , D effect is slightly more dominant than the ML test decreasing σ_h , showing smaller effect of loading damage in increasing σ_h (as compared with those performed at $\sigma_h = 0.25$ MPa). The results of the tests performed at $\sigma_h = 1.00$ MPa in Figure

4e shows that, in the ML test increasing σ_h , CL effect becomes more dominant than D effect due to the previous loading history.

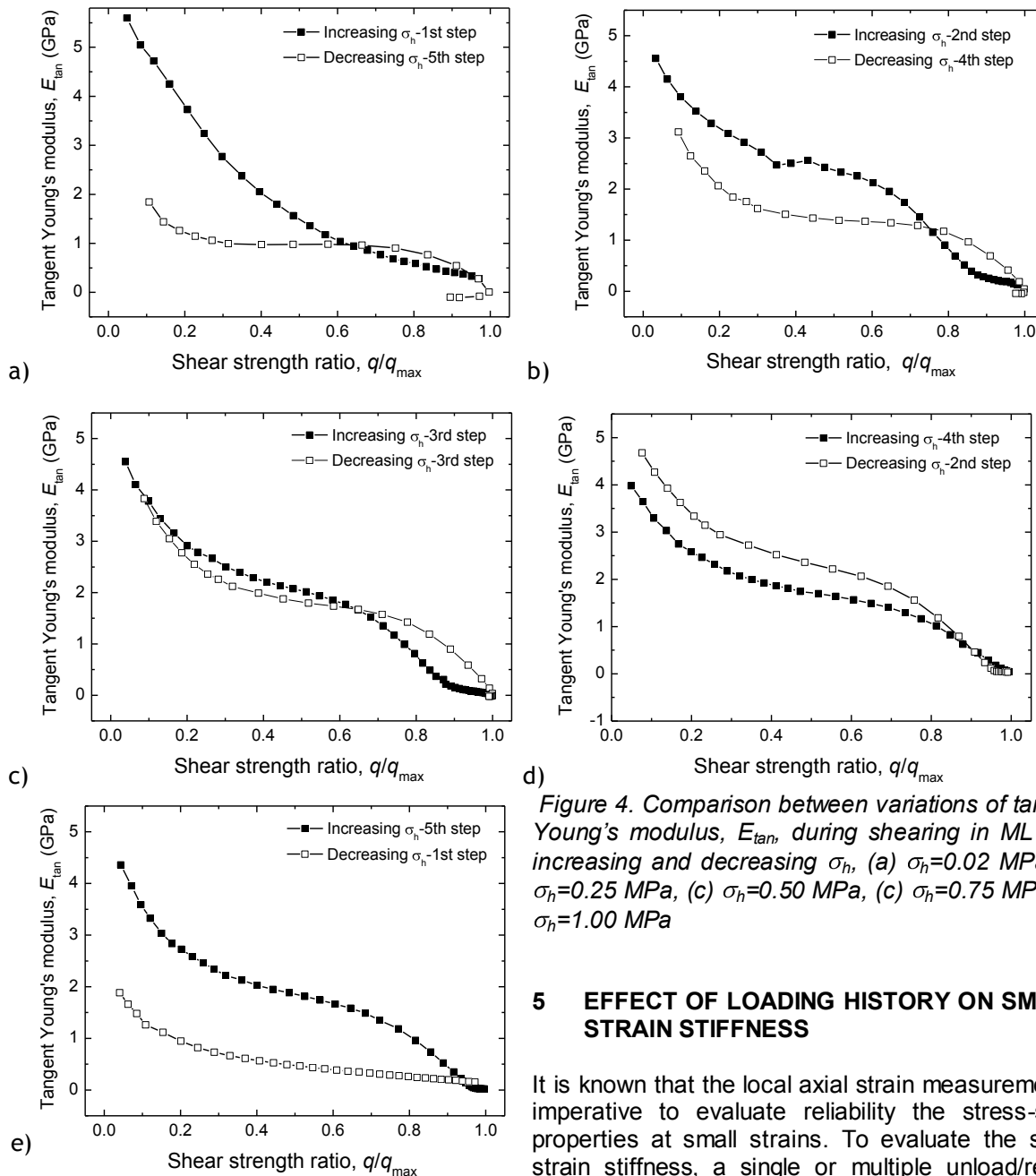


Figure 4. Comparison between variations of tangent Young's modulus, E_{tan} , during shearing in ML tests increasing and decreasing σ_h , (a) $\sigma_h=0.02$ MPa, (b) $\sigma_h=0.25$ MPa, (c) $\sigma_h=0.50$ MPa, (c) $\sigma_h=0.75$ MPa, (d) $\sigma_h=1.00$ MPa

5 EFFECT OF LOADING HISTORY ON SMALL-STRAIN STIFFNESS

It is known that the local axial strain measurement is imperative to evaluate reliability the stress-strain properties at small strains. To evaluate the small-strain stiffness, a single or multiple unload/reload cycle(s) with a single amplitude axial strain of a

order of 0.001% is usually applied at otherwise continuous TC loading, for example. In this study, such cyclic loading didn't apply during ML tests. However, it was noticed that, due to inherent drawback of the axial loading device, the axial strain rate for a very small axial strain range becomes very high immediately after the start of unloading. This fast unloading in an unload/reload step, is shown in Figure 5 for the ML test increasing σ_h . Taking advantage of this behaviour, the slope of very fast unloading part can be defined as a type of small-strain Young's modulus (E_d), close to the true elastic modulus (E_e). The effect of loading history on small-strain stiffness in terms of (E_d) during ML TC test increasing σ_h and decreasing σ_h is studied in this section.

Figure 6, shows the Young's modulus, E_d calculated for each loading step in ML tests increasing σ_h and decreasing σ_h , plotted against accumulative number of loading steps. In the ML test increasing σ_h , the specimen exhibits E_d values close to the truly elastic modulus, E_e . In this test, E_d values increase slightly with stepwise increase of σ_h , (i.e. deviator stress increase). On the other hand, in the ML test

decreasing σ_h , E_d increases first with an increase in deviator stress and then decreases. This reduction is significant in the last unloading step, showing the negative effect of irreversible shearing at previous loading on E_d values. This implies that, E_d value cannot be taken as an accurate representative of the truly elastic Young's modulus E_e , if the specimen is damaged by a loading history. Moreover, we can conclude that, damage effect may affect both large-strain and small-strain stiffness in ML test decreasing σ_h . This matter is more stressed for the results measured at low confining pressures where the specimen is stressed in a stress softening regime.

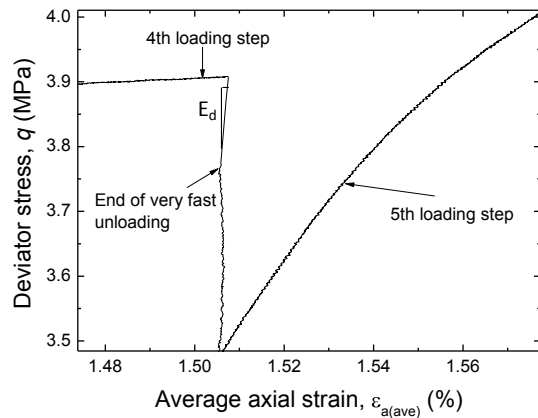


Figure 5. Very fast unloading at the end of the fourth loading step in the ML test increasing σ_h

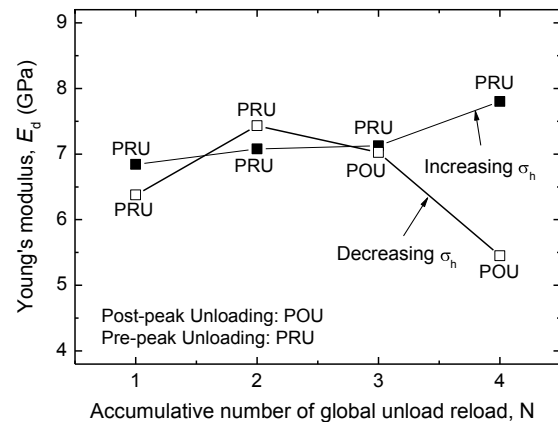


Figure 6. E_d values for ML tests increasing and decreasing σ_h

6 CONCLUSION

Effects of loading histories on the Tangent Young's modulus, E_{tan} , during multiple-step loading triaxial compression tests following increasing and decreasing confining pressures (σ_h s) were studied. Combined effects of three factors were identified: a) cyclic loading effects (CL effect); b) effects of pressure level on E_{tan} during primary loading and the one during reloading (P effect); and c) effect of damage that has taken place during preceding loading histories (D effect). In ML test increasing σ_h , CL effect was masked by P effect and D effect was negligible. However, in ML test decreasing σ_h , D effect was more significant. In this test, large D effect was also observed in small strain stiffness, E_d , values.

REFERENCES

- Anderson, W.F. (1974). "The use of multi-stage triaxial tests to find the undrained strength parameters of stony boulder clay." Proc. of Institute of Civil Engineering, Pt. 2, Vol. 57, Thomas Telford Ltd. London, 367-373.
- Aoki, H., Yonezawa, T., Watanabe, O., Tateyama, M., Tatsuoka, F. (2003). "Results from field full-scale loading tests on a bridge abutment with backfill of geogrid-reinforced cement-mixed gravel." Geosynth. Engrg. J., Japanese Chapter of International Geosynthetics Society, 18, 237-248 (in Japanese).
- Fortuna, S., Callisto, L., Rampello, S. (2006). "Small strain stiffness of a soft clay along stress paths typical of excavations." Proc. Soil Stress-Strain Behavior: Measurement, Modeling and Analysis Geotechnical Symposium in Rome.
- Goto, S., Tatsuoka, F., Shibuya, S., Kim, Y.S., Soto, T. (1991). "A simple gauge for local small strain measurements in the laboratory." Soils and Foundations, 31(1), 169-180.
- Jovicic, V., Coop, M.R. (1997). "Stiffness of coarse-grained soils at small strains." Géotechnique, 47, 357-362.
- JGS (2001). "Triaxial compression test on soft rock." Jap. Geotech. Standard, JGS 2533-2001.
- Kovari, K., Tisa, A. (1975). "Multiple failure state and strain controlled triaxial tests." Rock Mechanics, 7, 17-33.
- Tatsuoka, F., Kohata, Y., Ochi, K., Kim, Y.S., Shi, D. (1993). "Measuring small strain stiffness of soft rocks." Balkema, Geotechnical Engineering of Hard Soils – Soft Rocks.
- Tatsuoka, F., Hayano, K., Koseki, J. (2003). "Strength and deformation characteristics of sedimentary soft rock in the Tokyo metropolitan area." Proc. of Characterization and Engineering Properties of Natural Soils, Swets and Zeitlinger, 1461-1525.
- Tatsuoka, F., Nawir, H., Kuwano, R. (2004). "A modeling procedure of shear yielding characteristics affected by viscous properties of sand in triaxial compression." Soil and Foundations, 44 (6), 83-99.
- Tatsuoka, F., Hirakawa, D., Nojiri, M., Aizawa, H., Nishikiori, H., Soma, R., Tateyama, M., Watanabe, K. (2009). "A new type integral bridge comprising geosynthetic-reinforced soil walls." Geosynthetics International, IS Kyushu 2007 Special Issue, 16(4), 301-326.
- Wang, Y., Ng, C.W.W. (2005). "Effects of stress paths on the small-strain stiffness of completely decomposed granite." Can. Geotech. J. 42, 1200-1211.
- Watanabe, K., Tateyama, M., Jiang, G., Tatsuoka, F., Lohani, T. N. (2003). "Strength characteristics of cement-mixed gravel evaluated by large triaxial compression tests." Proc. 3rd Int. Conf. on Pre-Failure Deformation characteristics of Geomaterials (Di Benedetto et al., eds.), Lyon, Balkema, (1), 683-693.